RESEARCH PAPER

Measurement uncertainties of size, shape, and surface measurements using transmission electron microscopy of near-monodisperse, near-spherical nanoparticles

Pieter-Jan De Temmerman · Jeroen Lammertyn · Bart De Ketelaere · Vikram Kestens · Gert Roebben · Eveline Verleysen · Jan Mast

Abstract Transmission electron microscopy (TEM) in combination with a systematic selection procedure for unbiased random image collection, semi-automatic image analysis, and data processing has been validated for size, shape, and surface topology measurements of silica nanoparticles. The validation study, assessing the precision and accuracy of the TEM method, consists of series of measurements on two colloidal silica-certified reference materials, with number-based modal area-equivalent circular diameters (ECD) of 19.4 nm (ERM-FD100) and 27.8 nm (ERM-FD304). The measurement uncertainties are estimated for the modal and median particle size, shape, and surface topology parameters of single primary particles. The single primary particles are distinguished from agglomerates using a linear discriminant analysis approach. After optimization of the binning process, the mode associated with the number-based particle size distribution is obtained by lognormal fitting. The methodology described in this paper relies on a high level of automation of calibration, image acquisition, image analysis, and data analysis and gives robust results for the modal ECD. The expanded uncertainty of the modal ECD is estimated to be about 3 %. The largest contribution to the expanded uncertainty stems from the uncertainty associated with the trueness of the TEM method.

Keywords Transmission electron microscopy · Method validation · Reference material · Silica nanoparticles · Measurement uncertainty · Nanometrology

P.-J. De Temmerman · E. Verleysen · J. Mast (✉)
Service Electron Microscopy, Veterinary and Agrochemical Research Centre (CODA-CERVA), Groeselenberg 99, 1180 Brussels, Belgium
e-mail: jan.mast@coda-cerva.be

P.-J. De Temmerman
e-mail: pieter-jan.detemmerman@coda-cerva.be

E. Verleysen
e-mail: eveline.verleysen@coda-cerva.be

P.-J. De Temmerman · J. Lammertyn · B. De Ketelaere
Division MeBioS, Department of Biosystems, KULeuven, Willem de Croylaan 42, 3001 Leuven, Belgium
e-mail: jeroen.lammertyn@biw.kuleuven.be

B. De Ketelaere
e-mail: bart.deketelaere@biw.kuleuven.be

V. Kestens · G. Roebben
Institute for Reference Materials and Measurements (IRMM), Joint Research Centre, European Commission, Retieseweg 111, 2440 Geel, Belgium
e-mail: vikram.kestens@ec.europa.eu

G. Roebben
e-mail: gert.roebben@ec.europa.eu

Introduction

Recently, the European Commission (EC) adopted a Recommendation on the definition of a nanomaterial (NM) (EC 2011). For legislative and policy purposes in the European Union, this Recommendation should be used as basis for determining whether a material should be considered as a "nanomaterial" (SCENIHR 2010). The implementation of this definition relies on the availability of validated particle counting/imaging methods (EFSA 2011; OECD 2010).

TEM has been found to be a key method for characterizing various types of nanomaterials with sizes between 10 nm and 1 μm, including monodisperse types of silica, gold, and polystyrene latex nanoparticles which can be used for calibration, validation, and/or performance evaluation of particle sizing instruments (Pyrz and Buttrey 2008; Ehara and Sakurai 2010; Bau et al. 2010). For reliable and accurate quantitative analysis of nanoparticles present in representative TEM micrographs, a validated method is required. To date, TEM methods have only been rarely validated. As a result, the majority of today's nanomaterial characterization studies lack information that reflects the quality (i.e. measurement uncertainties) of the presented data. Reliably estimated measurement uncertainties are essential to underpin the credibility of experimental data and to compare TEM measurement results over time and space.

The capability of the TEM method to provide robust and accurate results of physical NM properties, such as particle size, shape, and surface topology depends on the type of material, on the preparation of a test specimen, and also on a number of image analysis parameters. A suitable sample preparation which does not change the primary particle size and shape is crucial to ensure that no additional size-fractionation occurs. The most relevant parameters are considered to be the sample preparation, the selection of particles on the micrographs, the number of measured particles, the data binning procedure, the applied magnification, and the calibration strategy of the microscope. Documentary standards ISO 13322 and ISO 9276 describe instructions for sample preparation, instrument operation, and image analysis (ISO 13322-1 2004; ISO 9276-3 2008; ISO 9276-1 1998). However, detailed procedures with respect to the choice of magnification, calibration, and data binning are not included in these standards.

In this paper, the use of TEM in combination with a systematic selection procedure for unbiased random image collection, semi-automatic image analysis, and data processing is evaluated for the measurement of selected physical properties of single primary particles. The accuracy of the TEM method is examined based on measurements performed on two colloidal silica-certified reference materials (CRMs). In addition to the uncertainties on the modal ECD of single primary particles, the uncertainties on the modal and median size, shape, and surface topology parameters are estimated.

Materials and methods

Reference materials

The accuracy of the presented TEM method is assessed using CRMs: ERM-FD100 and ERM-FD304. These CRMs consist of near-monodisperse, near-spherical nanoparticles suspended in an aqueous solution. The materials have been produced and supplied by the Institute for Reference Materials and Measurements (IRMM) of the Joint Research Centre (JRC) of the European Commission (Geel, Belgium). The CRMs have been certified in a transparent, detailed, and metrologically rigorous manner, and are primarily intended for quality control in daily laboratory practice, method development, and proficiency testing schemes.

These CRMs are certified for different equivalent diameters of the silica nanoparticles following multiple methods, including TEM and scanning electron microscopy (SEM). For ERM-FD100, the certified number-based modal diameter as established by TEM and SEM is 19.4 nm with a certified expanded uncertainty (coverage factor $k = 2$) of 1.3 nm (ISO 13322-1 2004; IRMM 2011). ERM-FD304 has certified values based on dynamic light scattering and centrifugal liquid sedimentation. However, a certified value for electron microscopy (SEM and TEM) is not assigned due to the low reproducibility obtained in the interlaboratory comparison part of the certification study (Franks et al. 2012). Consequently, only an indicative number-based modal diameter of 27.8 nm with an indicative expanded uncertainty (coverage factor $k = 2$) of 1.5 nm is available for ERM-FD304 (IRMM 2012).

Sample preparation and analysis

TEM specimens are prepared using the grid on drop method by bringing 10 µl of the diluted dispersion on pioloform- and carbon-coated, 400 mesh copper grids (Agar Scientific, Essex, England) that are pretreated with 1 % Alcian blue (Fluka, Buchs, Switzerland) to increase hydrophilicity as described in Mast and Demeestere (2009). ERM-FD100 is 1000 times diluted and ERM-FD304 is 100 times diluted in double distilled water. This water was home-made by twice distilling demineralized tap water.

The samples are imaged in bright field mode using a Tecnai Spirit TEM (FEI, Eindhoven, The Netherlands) with Biotwin lens configuration operating at 120 kV. Micrographs are recorded using a systematic selection procedure for unbiased random image collection as described in De Temmerman et al. (2012) using a 4*4 K CCD camera (Eagle, FEI). Briefly: micrographs are taken at positions pre-defined by the microscope stage and evenly distributed over the entire grid area. When the field of view was obscured, *e.g.* by a grid bar or an artifact, the stage was moved sideways to the nearest suitable field of view. The magnifications of 18,500 and 68,000 times are calibrated using the cross-grating method and the image shift method based on a 2,160 lines/mm optical diffraction-cross grating (Agar Scientific, Stansted, England). The calibration method is implemented following ASTM E766 guidelines (ASTM E766-98(2008)e1 2008) and by using the magnification calibration software which is integrated in the Tecnai user interface software (FEI).

Micrographs are analyzed using the iTEM software (Olympus, Münster, Germany). To prevent bias in the selection of the particles on the micrographs, and in line with (ISO 13322-1 2004), the particles on the lower and right hand side borders of the frame are omitted from analysis, as illustrated in Fig. 1.

Validation methodology

The precision part of the quantitative TEM method validation studies is based on determining repeatability (within one day variability) and intermediate precision (day-to-day variability) for measurements on ERM-FD100 and ERM-FD304. One sample of ERM-FD100 and one sample of ERM-FD304 are analyzed on five consecutive days. On each day, three

diluted aliquots are prepared from the original sample and three specimens are independently prepared from each aliquot (vial). From each specimen, TEM micrographs of 10 fields are recorded (De Temmerman et al. 2012) at two magnifications, namely 18,500 and 68,000 times, and analyzed (Appendix 1).

Identification of the measurands

Twenty-three measurands of size, shape, and surface topology are considered potentially relevant for the morphological characterization of the examined silica nanoparticles. Detailed information regarding these measurands can be found in De Temmerman et al. (2012). For each particle, these characteristic measurands are measured and the corresponding number-based distributions are obtained. The median values of the measurands are estimated for each sample and the distributions are constructed by binning the raw data on a linear abscissa. The width of the bins is manually altered until the number of non-empty bins is equal to the number of measurements in the largest bin (Fig. 2). The modes and full width at half maximum (FWHM) of the distributions of seven one-dimensional size measurands, namely ECD, Feret max, Feret mean, Feret min, diameter max, diameter mean, and diameter min, are determined for each dataset of 10 systematically selected TEM micrographs. This mode is defined as the position of the maximum of the log-normal function fitted to the distribution (Fig. 2). Iterative curve fitting of the log-normal distribution is performed using the Fityk software by selecting the Levenberg–Marquart algorithm (Wojdyr 2010). One-dimensional size measurements are compared by performing one-way analysis of variance and the Tukey test using sigmaplot (STATSCONsult, Drunen, The Netherlands) at a significant difference level of 0.05.

Working range

The useful working range of the TEM is defined by the lower and upper size quantification limits. The lower size quantification limit is calculated based on the work of Merkus (2009), who showed that large systematic deviations in size measurements can be avoided if the particle area consists of at least hundred pixels. The upper size quantification limit is restricted by the field of view and is set to one tenth of the image
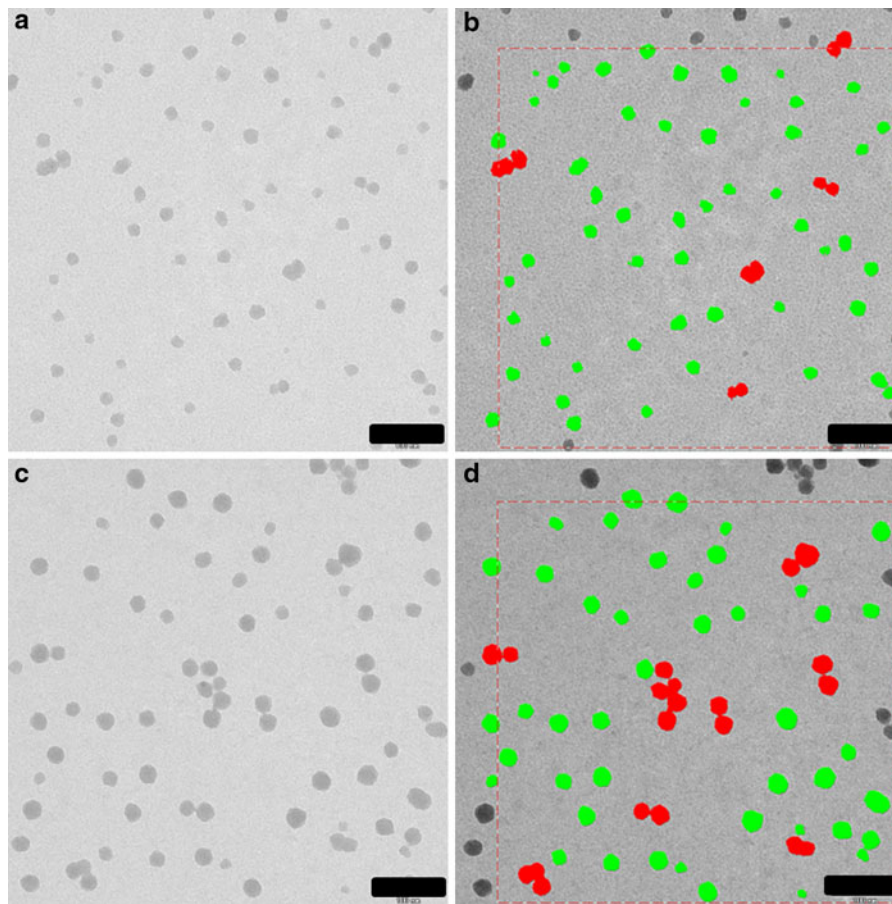
Fig. 1 Representative micrographs of ERM-FD100 and ERM-FD304 and illustration of the method of detection based on electron density and a measurement frame. The NM in the representative electron micrograps of ERM-FD100 (**a**) and ERM-FD304 (**c**) are detected, manually classified into single primary particles (*green*) and agglomerates (*red*) and false color-coded in the corresponding annotated images (**b**) and (**d**). The measurement frame (*dashed red line*) is placed at a distance from the top and left side which corresponds with 10 % of the width and height of the micrograph. The *bottom* and *right* side of the frame are set as rejected sides. Magnification 68,000, *bar* 100 nm. (Color figure online)

size as proposed in ISO 13322-1 (2004). The calculated working range and the corresponding magnification, pixel size, and size of the field of view are summarized in Appendix 2 for the magnifications of 18,500 and 68,000 times.

A preliminary experiment demonstrated that ERM-FD100 and ERM-FD304 are monomodal. No particles with an area smaller than 52 nm^2 are observed in the samples. Such an area corresponds to particles that contain 142 pixels at a magnification of 18,500 times and 2,000 pixels at a magnification of 68,000 times. For this reason, particles with an area smaller than 52 nm^2 (corresponding with an ECD of about 8 nm) are considered as background signal and are omitted from analysis.

Analysis and selection of single primary particles

Single primary particles can be automatically selected in the datasets of ERM-FD100 and ERM-FD304 based on their morphology using the following approach. The morphology of the single primary particles is characterized in a preliminary experiment. In 10 micrographs all detected and measured particles are manually classified, either as single primary particles or as agglomerates. In the generated subdataset, which contains only the classified single primary particles, a correlation matrix of all 23 measurands is set up. Measurands that describe the morphology of the single primary particles and which have a low correlation (<0.5) with the ECD are selected (Appendix 3). The

Fig. 2 Illustration of the binning and log-normal fitting of the number-based particle size distributions of ERM-FD100 (**a**) and ERM-FD304 (**b**). A subdataset of 146 measurements is randomly selected at a magnification of 18,500 times for each CRM
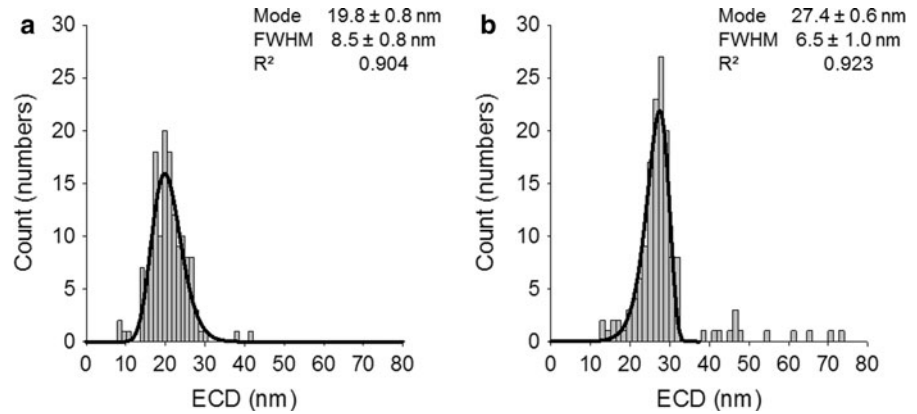
measurand showing the best separation between single and agglomerated primary particles is determined by performing linear discriminant analysis (LDA) on the full dataset.

The measurand with the lowest Type I and Type II classification errors (Appendix 4) is then considered for an automated classification in the other micrographs, resulting in a large dataset consisting of separated populations of single primary particles and agglomerates. The LDA calculations are programmed in the computational language "R" (R version 2.15.2, 2012) in RStudio (RStudio v 0.97, RStudio, Boston, MA, USA) which is available as freeware.

Robustness

The proposed method is inherently robust against "variation" introduced by the TEM operator because of a strong emphasis on the automation of the particle selection and image analysis aspects.

The robustness of the TEM method is assessed by varying the magnification and the number of analyzed particles which may influence the performance of the method. This magnification is varied between 18,500 and 68,000 times. The number of particles used to construct the number-based size distribution is varied by taking subdatasets. At a magnification of 68,000 times, the subdatasets contain between 3 and 335 particles and between 3 and 225 particles for ERM-FD100 and ERM-FD304, respectively. At a magnification of 18,500 times, the subdatasets contain between 3 and 4,050 particles and between 3 and 2,900 particles for ERM-FD100 and ERM-FD304, respectively. The effect of sample preparation is not

included in the robustness part of the present validation study. Care should, therefore, be taken not to extrapolate the conclusions of this study to TEM methods following significantly different sample preparation approaches.

Precision

The intra-laboratory precision (composed of repeatability and intermediate precision) of the quantitative TEM method is assessed by measurements performed on ERM-FD100 and ERM-FD304 similar to the test design described in Braun et al. (2011a). Repeatability indicates the closeness between results of measurements, performed over a short period, using the same instrument and performed by the same operator. The relative repeatability uncertainty is calculated from the dataset using Eq. 1. The mean sum of squares is calculated using one-way analysis of variance (ANOVA), with SoftCRM, an undated version of the software described in Bonas et al. (2003).

$$u(r) = \frac{\sqrt{\mathrm{MS_{within}}}}{C_m} \quad (1)$$

With $u(r)$ being the relative repeatability uncertainty, $\mathrm{MS_{within}}$ the mean of squares within the measurement days, and C_m the mean measured value. The relative intermediate precision uncertainty (day-to-day variability) is determined with Eq. 2:

$$u(\mathrm{ip}) = \frac{\sqrt{\frac{\mathrm{MS_{between}} - \mathrm{MS_{within}}}{n_r}}}{C_m} \quad (2)$$

With $u(\mathrm{ip})$ being the relative intermediate precision uncertainty, $\mathrm{MS_{between}}$ the mean sum of squares

between different days, and n_r the number of measurement replicates per day.

The relative intra-laboratory precision uncertainty is then determined by combining the relative repeatability uncertainties and the relative intermediate precision (Eq. 3).

$$u(\text{lab}) = \sqrt{u^2(r) + u^2(\text{ip})} \qquad (3)$$

The intra-laboratory precision uncertainty summarizes the uncertainties related to the non-systematic variability in sample preparation, image acquisition, image analysis, and data analysis.

Uncertainty of the estimation of the mode

The uncertainty related to the estimation of the mode from the raw dataset, $u(\text{mode})$, is concealed in the repeatability and intermediate precision. Amongst all contributions to repeatability and intermediate precision, $u(\text{mode})$ is the one that depends most directly on the number of measured particles. It is, therefore, proposed to evaluate the $u(\text{mode})$ by separating the intra-laboratory precision uncertainty into a part which is dependent on the number of measured particles, $u(\text{mode})$, and a part which is independent on the number of measured particles, $u'(r)$ and $u'(\text{ip})$ (Eq. 4).

$$u(\text{lab}) = \sqrt{u^2(\text{mode}) + u'^2(r) + u'^2(\text{ip})} \qquad (4.)$$

With $u'(r)$ and $u'(\text{ip})$ being the uncertainties which do not depend on the number of measured particles. Subdatasets on a logarithmic scale (Fig. 3) are taken each day and for each repetition. For each subdataset, the laboratory uncertainty is determined. Linear regression is performed on the logarithmic plot of the laboratory uncertainty as a function of the sample size.

Calibration

The calibration of the microscope magnification using the cross-grating method and the image shift method is performed following ASTM E766 guidelines. The uncertainty associated with calibration, $u(\text{cal})$, is considered to be about 0.1 and 1.3 % for magnifications of 68,000 and 18,500 times, respectively.

Trueness

The results of a method are "true" if the method is free of systematic and significant bias. Whether a method produces significantly biased results can be assessed by comparing the results with reference values, for example by measuring one or more suitable CRMs as described in ERM application note 1 (Linsinger 2010). When the combined uncertainty of the measurement results and the certified value are larger than the absolute difference between the certified and the measured value (Δ_m), then it can be concluded that the measured value is not significantly different from the certified value. If the opposite is the case, then the method results are significantly biased and a correction of the results is preferred. Instead one can also choose to include the measured bias in the measurement uncertainty, especially when the bias value is not very well known.

This trueness assessment is not free of uncertainty itself, so even if the assessment indicates that the results are without significant bias, an uncertainty associated with the assessment of the trueness of the method must be taken into account. The trueness uncertainty, $u(t)$, can be calculated by combining the uncertainty of the measurements on the CRMs, $u(m)$, with the uncertainties of the certified values of the CRMs, $u(\text{CRM})$ (Eq. 5)

$$u(t) = \sqrt{u^2(m) + \frac{\sum u^2(\text{CRM})}{n_{\text{CRM}}^2}} \qquad (5)$$

With $\sum u^2(\text{CRM})$ being the sum of the squares of the relative uncertainties of the certified values of the CRMs and n_{CRM} the number of CRMs.

In validation studies, such as the study presented in this paper, the uncertainty $u(m)$ of the results obtained on the CRMs is usually not a full measurement uncertainty, as it does not yet contain the $u(t)$ contribution. Instead, $u(m)$ contains repeatability and intermediate precision uncertainty contributions and can be estimated from Eq. 6

$$u(m) = \sqrt{\frac{u^2(r)}{n_t} + \frac{u^2(\text{ip})}{n_d}} \qquad (6)$$

With $u(\text{ip})$ being the relative intermediate precision uncertainty, $u(r)$ the relative repeatability uncertainty, n_d the number of test days, and n_t the total number of
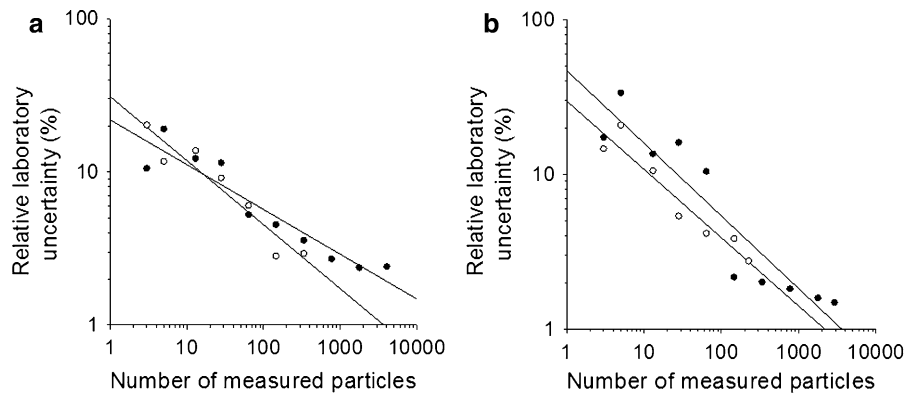
Fig. 3 Correlation between the relative laboratory uncertainty and the number of measured particles per repetition. The linear regression between the log transformation of the relative laboratory uncertainty and the log transformation of the number

of measured particles per repetition for ERM-FD100 and ERM-FD304 at magnifications of 18,500 (*filled circle*) and 68,000 times (*unfilled circle*) are given in (**a**) and (**b**), respectively

measurement replicates. Note that the precision contributions to $u(m)$ are different from those to $u(\text{lab})$ because the number of replicates and measuring days in the validation study is higher than during routine use of the method. Also, since two CRMs are tested, the measurement uncertainty of the technique is calculated from the average of the relative repeatability and relative intermediate precision uncertainties of measurements of the two CRMs.

Only for ECD the trueness uncertainties of TEM analyses can be estimated using the certified uncertainty of ERM-FD100 and the indicative uncertainty of ERM-FD304.

Combined and expanded measurement uncertainty

The uncertainty contributions explained above are to be combined in the method's full uncertainty budget. The intra-laboratory precision uncertainty $u(\text{lab})$ is a type A uncertainty: it is derived from repeated testing and covers all sources of variation between analyses and the typical between-day variation. A type B uncertainty component (values taken from certificates, expert judgement, etc.) is the uncertainty of the certified values of the used CRMs, $u(\text{CRM})$, and the calibration uncertainty, $u(\text{cal})$. The trueness uncertainty $u(t)$ is a mix of A and B type uncertainties (ISO/IEC GUIDE 98-3 2008).

If one assumes that all the uncertainty contributions of the quantitative TEM method are covered by the intra-laboratory precision uncertainty and the uncertainties for

trueness and calibration, then the combined measurement uncertainty can be estimated from (Eq. 7):

$$u_{\text{c}}(x) = \sqrt{u^2(\text{lab}) + u^2(t) + u^2(\text{cal})} \qquad (7)$$

The uncertainties are combined using the normal root-sum-square manner, resulting in the combined measurement uncertainty $u_{\text{c}}(x)$. By assuming that the combined uncertainty is normally distributed and a confidence level of approximately 95 % is required, and when the degrees of freedom of the individual uncertainty contributions permit, the combined uncertainty can be multiplied by a coverage factor (k) of 2 to obtain the expanded measurement uncertainty $U(x)$ (ISO/IEC GUIDE 98-3 2008).

Results

Selection of single primary particles

The size, shape, and surface characteristics of single particles and agglomerates of ERM-FD100 and ERM-FD304 are bimodally distributed. This is illustrated in Appendix 5 for the sphericity measurand. The largest peak of the number-based distribution corresponds to the single primary particles and the second peak corresponds to the agglomerated particles.

In this validation study, only single primary particles are considered. As illustrated in Appendix 3, the aspect ratio, convexity, elongation, shape factor, and sphericity measurands have a low correlation (less than 0.5)

with ECD. From these measurands, the sphericity allows to separate single primary particles from the agglomerates with the lowest type I and type II uncertainties as illustrated in Appendix 4. With this separation about 1 % of the single primary particles are removed from the datasets and about 1 and 5 % of the agglomerates are classified as single primary particles for ERM-FD100 and ERM-FD304, respectively.

The measured modal sphericities of the single primary particles of both ERM-FD100 and ERM-FD304 are about 0.8 and confirm that the particles of these materials are approximately spherical. Particles that have a sphericity lower than 0.4 for ERM-FD100 and lower than 0.5 for ERM-FD304 are classified as non-spherical particles (Appendix 5). Since the primary particles of ERM-FD304 are more homogeneous, a stricter threshold can be used for ERM-FD304 than for ERM-FD100. For ERM-FD100 the percentage of agglomerated particles is lower than that for ERM-FD304 (Table 1). The number-based size distributions of Feret max, Feret mean, Feret min, ECD, diameter max, diameter mean, and diameter min of the single primary particles are shown in Fig. 4 and Appendix 6 and the corresponding modes and FWHMs in Table 2 and Appendix 7 at magnifications of 18,500 and 68,000 times, respectively.

Precision

The number of particles per micrograph decreases with increased (squared) magnification: in 150 micrographs about 12–14 times more particles are measured at a magnification of 18,500 times than at a magnification of 68,000 times. For ERM-FD100 a total of 102,276 and 7,403 single particles and for ERM-FD304 a total of 60,772 and 5,141 single particles are analyzed at magnifications of 18,500 and 68,000 times, respectively (Table 1).

Figure 5 shows the individual components of the uncertainty of TEM measurement of the mode of ECD of ERM-FD100 and ERM-FD304. Table 2 and Appendix 7 indicate that for all seven size measurands and for both ERM-FD100 and ERM-FD304, the intra-laboratory precision (the combined repeatability and intermediate precision) is better at a magnification of 18,500 times than at a magnification of 68,000 times.

As illustrated in Fig. 3, there is a linear relationship between the log-transformed relative laboratory uncertainty of the mean mode, and the log-

Table 1 Overview of the number of analyzed single and agglomerated particles in 150 micrographs for ERM-FD100 and ERM-FD304 at magnifications of 18,500 and 68,000 times

Nanomaterial	ERM-FD100		ERM-FD304	
Magnification	18,500	68,000	18,500	68,000
Single particles	102,276 (86 %)	7,405 (87 %)	60,772 (69 %)	5,141 (74 %)
Agglomerates	16,353 (14 %)	1,114 (13 %)	26,827 (31 %)	1,765 (26 %)

transformed of the number of measured particles. This linear relationship is shown in Eq. 8.

$$\text{Log}(N) = -\alpha \log(u(\text{lab})) + \log(\beta) \qquad (8)$$

The experimentally determined values for α and β and the minimal sample size N that is required to have a relative laboratory uncertainty lower than 0.05 are presented in Table 3.

The EC definition is based on the true median size value of the particle size distribution (EC 2011). Therefore, in addition to the calculation of the intra-laboratory precision for the modes, the intra-laboratory precision is also calculated for the median values (Appendix 8 and 9). The intra-laboratory precision uncertainty is combined with the calibration uncertainty to calculate the combined uncertainty. Since, for two-dimensional size, shape, and surface topology measurands, no reference values are available yet, the mean median value with its standard deviation and its combined intra-laboratory precision can be calculated for these measurands, but trueness cannot be assessed. As illustrated in Appendix 10, the combined intra-laboratory precision uncertainties of the measured median values obtained for all 23 measurands showed to be better at a magnification of 18,500 times than at a magnification of 68,000.

Trueness and combined measurement uncertainty

Table 4 shows the uncertainty components of the modes of the ECD size distributions measured by TEM. The trueness uncertainty is the largest uncertainty factor of the TEM measurement of the mean modal ECD; it is larger than the combined intra-laboratory uncertainty obtained when measuring ERM-FD100 and ERM-FD304 (Table 3). The relative combined uncertainties range from 3.5 to 4.5 % for ERM-FD100 and from 2.5 to 4.0 % for ERM-FD304.

Fig. 4 Number-based size distributions of ERM-FD100 (**a**) and ERM-FD304 (**b**) at a magnification of 18,500 times. The reported fittings are based on the mean values of the mode and FWHM in Table 2
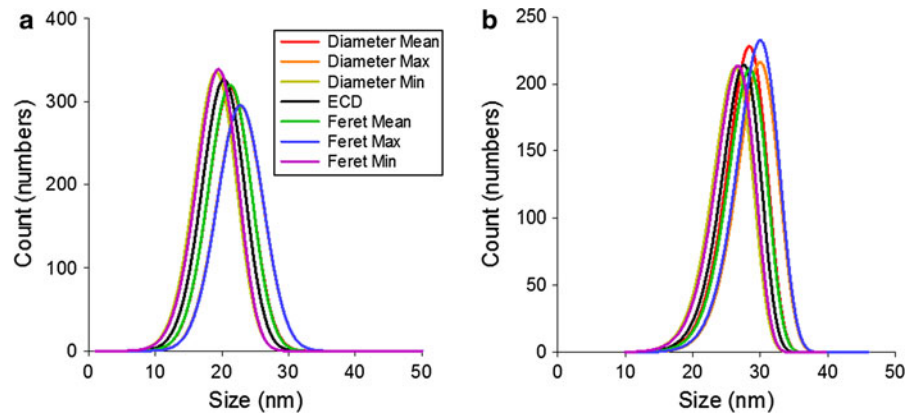
Table 2 Primary particle mean mode and full width at half maximum (FWHM) of the number-based size distributions and the corresponding intra-laboratory uncertainty u(lab) for ERM-FD100 and ERM-FD304 at a magnification of 18,500 times

	ERM-FD100		ERM-FD304	
	Mode $\pm$ u(lab)	FWHM $\pm$ u(lab)	Mode $\pm$ u(lab)	FWHM $\pm$ u(lab)
Diameter mean	21.2 $\pm$ 0.4 nm[a]	7.6 $\pm$ 0.4 nm[a]	28.4 $\pm$ 0.4 nm[a]	6.8 $\pm$ 0.3 nm[a]
Diameter max	22.7 $\pm$ 0.4 nm[b]	8.2 $\pm$ 0.4 nm[b]	30.0 $\pm$ 0.4 nm[b]	7.2 $\pm$ 0.4 nm[b]
Diameter min	19.1 $\pm$ 0.4 nm[c]	7.4 $\pm$ 0.4 nm[a]	26.3 $\pm$ 0.4 nm[c]	6.9 $\pm$ 0.3 nm[a]
ECD	20.3 $\pm$ 0.5 nm[d]	7.5 $\pm$ 0.4 nm[a]	27.5 $\pm$ 0.4 nm[d]	6.7 $\pm$ 0.3 nm[a]
Feret mean	21.2 $\pm$ 0.4 nm[a]	7.6 $\pm$ 0.4 nm[a]	28.4 $\pm$ 0.4 nm[a]	6.8 $\pm$ 0.3 nm[a]
Feret max	22.8 $\pm$ 0.4 nm[b]	8.1 $\pm$ 0.4 nm[b]	30.0 $\pm$ 0.4 nm[b]	7.2 $\pm$ 0.4 nm[b]
Feret min	19.4 $\pm$ 0.4 nm[c]	7.3 $\pm$ 0.3 nm[a]	26.7 $\pm$ 0.4 nm[c]	6.8 $\pm$ 0.3 nm[a]

[a,b,c,d] Different letters indicate significant different mean values by one-way analysis of variance and Tukey test ($p < 0.05$)

A better estimation of the trueness uncertainty can be calculated by combining the relative measurement uncertainty with the relative uncertainties from the two CRMs. The relative measurement uncertainty is then calculated by taking the average relative repeatability uncertainty and average relative intermediate precision uncertainty. As illustrated in Table 5 the combined uncertainty of the TEM measurement of the mode of the ECD is then about 3 %.

The absolute difference between the mean modal ECD-certified values and the measured modal ECD result is smaller than the expanded uncertainty for ERM-FD100 and ERM-FD304 for both 18,500 and 68,000 times magnifications (Table 4). The modes of the diameter min and Feret min are not significantly different from the certified ECD value of ERM-FD100 and diameter mean and Feret mean are not significantly different from the certified ECD value of ERM-FD304

(data not shown). Pair-wise comparison within our experiments shows that the modes of Feret min, ECD, Feret mean, and Feret max distributions are increasing and significantly different. The modes of diameter min, ECD, diameter mean, and diameter max distributions are equally increasing and significantly different. The respective minimum, median, and maximum values are similar for all Feret and diameter measurands. The widths of the Feret max and diameter max distributions are significantly larger than the widths of the distributions of the other size measurands.

Discussion

Transmission electron microscopy is considered a key method for NM characterization because of its high resolution (Linsinger et al. 2012). In this paper, TEM
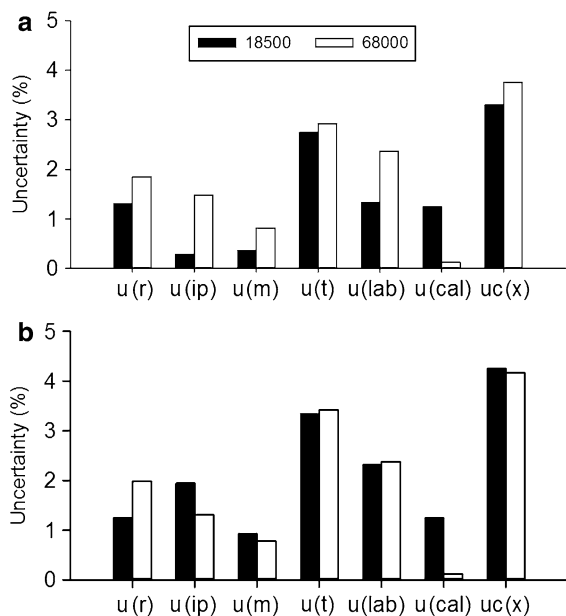
Fig. 5 Uncertainties of the TEM measurement of the mode of the ECD of ERM-FD100 (**a**) and of ERM-FD304 (**b**) at magnification of 18,500 (*black*) and 68,000 times (*white*)

Table 3 Characteristics of the linear regression between the log transform of the number of measured particles and the log transform of the relative laboratory uncertainty

Sample	α	β	N^a	R^2
ERM-FD100 68000	2.2	0.1	73	0.91
ERM-FD100 18500	3.1	0.02	149	0.89
ERM-FD304 68000	2.1	0.1	53	0.92
ERM-FD304 18500	1.9	0.4	114	0.87

[a] Number of particles that need to be measured to obtain a laboratory uncertainty smaller than five percent

analysis of colloidal silica CRMs is used to quantify the accuracy and precision of TEM size and shape measurements of near-monodisperse, near-spherical silica nanoparticles. An intra-laboratory validation study is reported for the TEM measurement of the modes of the ECD, diameter, and Feret single primary particle sizes and for the median values of 23 primary particle measurands, describing the size, shape, and surface properties of the colloidal silica materials.

The trueness uncertainty is the largest factor in the uncertainty budget of the measurement of the modal ECD of the silica materials. This trueness uncertainty consists mainly of the reported standard uncertainty of the certified value, which is 6–8 times larger than the

measured within-lab standard uncertainty of the mean values of the modes. Consequently, when TEM results need to be compared between different laboratories, e.g. in the context of mutual control of material suppliers, customers, and regulators, or in the context of characterizing reference materials, insisting on the standardization of the TEM methodology of the contributing laboratories (Roebben et al. 2013) is more effective than increasing the number of analyzed particles and repetitions in each laboratory.

The sample preparation, sampling of the TEM grid surface, image analysis, and the separation of single and agglomerated primary particles are important elements of standardized, quantitative TEM analyses. The ISO standards for TEM analysis of nanoparticles (ISO 13322-1 2004; ISO 9276-6 2008; ISO 9276-2 2001) do not always cover these elements in detail, mainly because they are very material-dependent. In this work, the uncertainties associated with these elements are examined.

Sample preparation

The silica particles of the investigated CRMs are negatively charged at physiological pH (Braun et al. 2011b; Franks et al. 2012). Hence, attachment and an even distribution on the EM grids could be assured by introducing positive charges on the grid surface using Alcian blue pretreatment. The systematic selection procedure for unbiased random image collection is applied to take into account the variation due to selection of the micrographs. This variation is included in the repeatability and intermediate precision (Russ 2011).

Automation of image analysis

Automation of the image analysis process allows measuring multiple and arithmetically complex measurands, described in De Temmerman et al. (2012), on ten thousands of detected particles. This automation reduces the operator-induced bias, avoids the tedious repeated task of manual measurement, and assures a statistically relevant number of measurements (Pyrz and Buttrey 2008).

The separation of isolated and agglomerated primary particles strongly influences the precision of the measurement of all measurands. For agglomerated nanoparticles, (Russ 2011) and (Pons et al. 1999)

Table 4 The absolute standard and expanded measurement uncertainties (nm) of modal ECD measurands obtained for ERM-FD100 and ERM-FD304 at magnifications of 18,500 and 68,000 times

Magnification	ERM-FD100		ERM-FD304	
	18,500 times	68,000 times	18,500 times	68,000 times
Mean measured value, C_m	20.26	19.54	27.54	26.71
Standard deviation[a]	0.44	0.45	0.37	0.61
Certified value, C_{CRM}^b	19.40	19.40	27.80	27.80
Standard uncertainty of certified value, u(crm)	0.65	0.65	0.75	0.75
Intra-laboratory precision, u(lab)[c]	0.47	0.47	0.37	0.63
Trueness, $u(t)$[d]	0.68	0.66	0.76	0.78
Calibration uncertainty, u(cal)[e]	0.25	0.02	0.34	0.03
Combined uncertainty, $u_c(x)$[f]	0.86	0.81	0.91	1.01
Expanded uncertainty, $U(x)$[g]	1.72	1.63	1.82	2.01
Δm[h]	0.86	0.14	0.26	1.09
$U(x)$-Δm[i]	0.86	1.49	1.56	0.92

[a] The standard deviation on the measured value

[b] Certified values are only available for the equivalent spherical diameter. It is assumed that these values are very similar to the other size measures

[c] u(lab) is the combined uncertainty of the repeatability and intermediate precision standard uncertainties

[d] $u(t)$ is the combined uncertainty of the measurement uncertainty and the uncertainty on the certified value

[e] u(cal) represents the calibration uncertainty

[f] $u_c(x)$ is the combined uncertainty of the intra-laboratory, trueness, and calibration uncertainties

[g] Δm is the absolute difference between the mean measured value and the certified value

[h] $U(x)$ is the combined uncertainty corresponding to a confidence interval of approximately 95 %. It is obtained by multiplication of $u_c(x)$ by a coverage factor (k) of 2 (ISO/IEC GUIDE 98-3 2008)

[i] To evaluate the method performance, Δm is compared with $U(x)$ values. If $\Delta m \leq U(x)$, i.e., $U(x)$—$\Delta m > 0$, then there is no significant difference between the measurement result and the certified value

suggest a separator filter-based approach. This approach allows including primary particles in agglomerates but it can also introduce important distortions in the shape and size of the detected particles. Since already more than 70 % of the measured particles of the materials tested in this study are isolated primary particles, this population is supposed to be representative for the large majority of primary particles in the sample. The applied linear discriminant analysis approach proves to be effective in objectively selecting the best measurand for omitting the agglomerated particles. Only one to five percent of the agglomerates are defined as primary particles. From the non-size-related measurands, the sphericity measurand is shown to be the most efficient measurand separating agglomerated primary particles from isolated primary particles.

Since the CRM samples contain much more elongated than circular agglomerates, this sphericity-based separation is prefered over the shape factor-based separation, suggested by NIST (Kaiser and Watters 2007). The latter efficiently removes circular agglomerates but it tends to fail in removing small elongated agglomerates. These two approaches can be combined and the biparametric separation can be better than the uniparametric separation (data not shown). In this work, it is not applied because it requires complex iterative data processing.

Choice of magnification

The selection of an appropriate magnification and the limitation of image processing steps by applying an $N \times N$ filter minimizes the repeatability and intermediate precision uncertainties (Pyrz and Buttrey 2008). At the lower magnification (18,500 times), the intra-laboratory uncertainty is lowest even though the individual particles are less accurately measured (Pyrz and Buttrey 2008).

Table 5 Relative uncertainties (in %) of the TEM measurement and trueness estimation of the mode of the ECD at magnifications of 18,500 and 68,000 times

	18,500 times	68,000 times
Repeatability uncertainty, $u(r)$		
ERM-FD100	1.2	2.0
ERM-FD304	1.3	1.8
Average	1.3	1.9
Intermediate precision uncertainty, $u(ip)$		
ERM-FD100	1.9	1.3
ERM-FD304	0.3	1.5
Average	1.1	1.4
Measurement uncertainty, $u(m)$	0.6	0.8
Standard uncertainty of certified value, $u(CRM)$		
ERM-FD100	2.7	2.7
ERM-FD304	3.4	3.4
Trueness uncertainty, $u(t)$[a]	2.2	2.3
Laboratory uncertainty, $u(lab)$[b]	1.7	2.4
Calibration uncertainty $u(cal)$[c]	1.3	0.1
Combined uncertainty, $u_c(x)$[d]	3.1	3.3

[a] $u(t)$ is the combined uncertainty of the measurement uncertainty and the uncertainty on the certified value

[b] $u(lab)$ is the combined uncertainty of the average repeatability and average intermediate precision uncertainties

[c] $u(cal)$ represents the calibration uncertainty

[d] $u_c(x)$ is the combined uncertainty of the intra-laboratory, trueness, and calibration uncertainties

Indeed, more particles are detected per micrograph and the selection bias is lower than at the higher magnification of 68,000 times. At the magnification of 18,500 times, the lower intra-laboratory uncertainty is, however, compensated by the higher calibration uncertainty resulting in similar combined intra-laboratory uncertainties of the analyses at magnifications of 18,500 and 68,000 times. At the lower magnification small surface features could be underestimated. This should be taken into account for complex nanomaterials. However, in the examined silica CRM qualitative TEM analyses at high magnifications did not suggest the presence of such surface features.

The cross-grating calibration method used for magnifications up to 18,500 times is less effective than the image shift calibration method used for higher magnifications. Application of the latter method on the magnification of 18,500 times is expected to lower the calibration uncertainty systematically with 1.1 %, but requires adaptation of the applied calibration software (FEI 2012). Since the uncertainty associated with the calibration procedure is added as a Type B uncertainty and is not covered by the intra-laboratory uncertainty, such improvements in the calibration procedure can be included in the method validation dossier without repeating the validation experiment (ISO/IEC GUIDE 98-3 2008).

Number of particles to be counted

Our experimental data show an approximately linear relationship between the log-transformed intra-laboratory precision uncertainty and the log-transformed number of measured particles, for small numbers of particles (<200). This is in agreement with ISO (ISO 13322-1 2004) and the simulations of (Masuda and Gotoh 1999) who postulate that there is a linear relationship between the log-transformed number of measured particles and the log-transformed uncertainty. For larger particle numbers, this intra-laboratory precision uncertainty becomes independent of the number of measured particles and is mainly determined by a particle number-independent part of the repeatability and intermediate precision uncertainties.

To achieve a relative laboratory uncertainty of 5 % at a confidence level of 95 % on the estimation of the mode, between 50 and 200 particles have to be measured. These numbers are in the same order of magnitude as the numbers calculated following the method of (Masuda and Gotoh 1999) proposed by ISO 13322-1 (2004) when assuming that the size is log-normally distributed.

Data binning and fitting of the resulting distributions

The data binning procedure (weighing the number of non-empty bins to the number of measurements in the largest bin), followed by log-normal fitting allows precise estimation of the mode. This way, the uncertainty of the measurement of the mode (bin width) and the number of particles supporting the measurement of the mode (bin height) are better balanced, certainly for non-normal distributions, than with the Freedman–Diaconis rule, the Scott's rule, and the Sturges rule,

designed for normal distributed data (Freedman and Diaconis 1981; Scott 2009, 2010).

Log-normal fitting to determine the mode decreases the repeatability and intermediate precision uncertainties of the mean modal ECD more than the estimation of the modal ECD based on the selection of the bin containing most particles (data not shown).

Comparison of different measurands characterizing the particle distributions

For the measured silica materials (near-monodisperse, near-spherical, and non-agglomerated) the mean modal sizes and mean median sizes and their corresponding uncertainties are comparable and can be used in function of the measurement purpose. In the scope of the EC nanomaterial definition the most relevant measure is the Feret min, an estimate of the minimal size in one dimension. A material qualifies as a NM when the median Feret min dimension is smaller than 100 nm (Linsinger et al. 2012; EC 2011). For comparison with literature data (Braun et al. 2011b; Franks et al. 2012) and for validation purposes, the mean modal values are applied as more robust estimators for size, shape, and surface topology measures of materials such as the colloidal silica materials studied here. The modal values are less sensitive to outliers in the dataset than the median values (Braun et al. 2011b; Franks et al. 2012).

The semi-automatic analysis allows accessing multiple measurands and selecting the optimal measurand in function of a specific material or measurement purpose. The shape measurements confirmed that the CRMs are colloids of near-spherical nanoparticles. The measured modal ECD value is similar to the certified ECD values. The Feret and diameter sizes are significantly different from the ECD values of the CRMs such that a specific certification of these measurands appears necessary (Linsinger et al. 2012). The effects of TEM sample preparation, by the combined action of drying and high vacuum, can supposed to be low (Linsinger et al. 2012) for the examined materials since a good agreement between the ECD size measured by TEM and the equivalent spherical diameter size measured by other techniques, such as centrifugal liquid sedimentation and even

dynamic light scattering, is observed (Braun et al. 2011b; Franks et al. 2012).

Validity range

The measurement uncertainties are determined for two silica NM and, since the particle detection is based on mass and thickness contrast, similar or better results are to be expected for similar particles, composed of heavier elements that can be more easily distinguished from the background. Earlier, this method allowed detecting and measuring colloidal silver (Klein et al. 2011) and gold NM (Van Doren et al. 2011).

Sensu stricto, the method is validated on near-monodisperse nanoparticles with a modal size in the range of 18–30 nm. In practice, the quantification limit of the applied microscope and camera configuration allows to detect and accurately measure particles with a diameter ranging from 10 to 400 pixels.

The determined measurement uncertainties are valid for near-spherical nanoparticles only. For nanoplates and nanofibres, like nanotubes, nanorods, and nanowires (ISO/TS 27687 2008), the size measurements depend on the orientation of the particles on the grid and, therefore, a separate validation is necessary.

Conclusions

This paper describes the validation of an in-house TEM method for the determination of the modal and median particle size, shape, and surface topology of near-monodisperse distributions of near-spherical colloidal silica primary particles. Uncertainty budgets for the TEM method are set up using data obtained on two CRMs. A high level of automation of the calibration, image acquisition, image analysis, and data analysis is obtained. This method proves to give precise and non-biased results for the modal particle ECD measurements of near-monodisperse populations of near-spherical nanoparticles in the size range between 18 and 30 nm. The expanded uncertainties on the modal ECDs are about 3 % and are mainly determined by the inter-laboratory component of the combined uncertainty of the reference materials. The expanded uncertainty can be applied to other colloidal near-spherical NM with

another composition on the condition that the primary particles can be distinguished from the background, and have a near-monodisperse size distribution. The presented sample preparation, calibration, image acquisition, image analysis, and data analysis can serve as a guideline to set up further validation experiments for TEM analyses of these and other NM.

Conflict of interest   The author(s) declare that they have no competing interests.

Appendix 1

See Fig. 6.
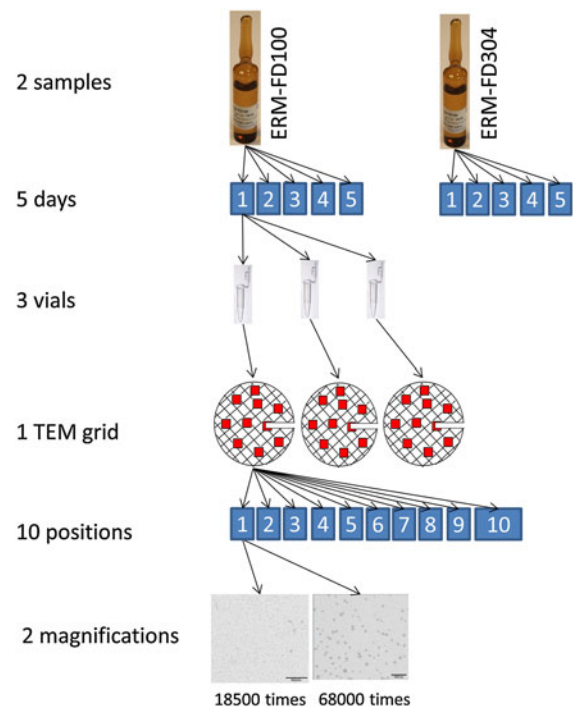
Fig. 6 Schematic overview of the experimental setup

Appendix 2

See Table 6.

Table 6 Overview of the pixel size and the size of the field of view, together with the corresponding lower and upper primary particle size quantification limits at magnifications of 18,500 and 68,000 times

Magnification	Lower size limit (nm)	Upper size limit (nm)	Pixel size (nm)	Field of view (nm)
18,500	6	245	0.6	2,450
68,000	2	66	0.2	660

Appendix 3

See Table 7.

Table 7 Correlation of the 23 measurands with the ECD size measurand, measured in a subdataset containing only single primary particles of ERM-FD100 and ERM-FD304 at magnifications of 18,500 and 68,000 times

	ERM-FD100		ERM-FD304	
Magnification	18,500	68,000	18,500	68,000
Diameter mean	0.99	0.98	1.00	1.00
Diameter max	0.99	0.96	0.98	0.98
Diameter min	0.99	0.97	0.98	0.98
ECD	1.00	1.00	1.00	1.00
Feret mean	0.99	0.99	1.00	1.00
Feret max	0.99	0.96	0.98	0.98
Feret min	0.99	0.97	0.98	0.98
Central distance mean	1.00	1.00	1.00	1.00
Central distance max	0.98	0.93	0.98	0.97
Central distance min	0.84	0.80	0.97	0.96
Radius of inner circle	0.71	0.93	0.98	0.98
Perimeter	0.89	0.83	1.00	0.98
Area	0.88	0.99	0.99	1.00
Convex area	0.86	0.97	0.99	0.99
Convex perimeter	0.99	0.99	1.00	1.00
Rectangle mean	0.86	0.96	0.99	0.99
Rectangle max	0.86	0.96	0.98	0.99
Rectangle min	0.86	0.96	0.98	0.99
Aspect ratio	**0.05**	**0.20**	**−0.20**	**−0.13**
Convexity	**−0.42**	**0.29**	**0.41**	**0.29**
Elongation	**0.08**	**0.23**	**−0.20**	**−0.14**
Shape factor	**−0.47**	**0.13**	**0.15**	**−0.09**
Sphericity	**−0.07**	**−0.20**	**0.22**	**0.15**

Cells marked in bold indicate measurands that have a correlation between −0.50 and +0.50 with the ECD

Appendix 4

See Table 8.

Table 8 Type I and Type II separation errors related to the uniparametric linear discriminant analysis of single primary particles and agglomerates in ERM-FD100 and ERM-FD304

Nanomaterial	ERM-FD100				ERM-FD304			
Magnification	18,500		68,000		18,500		68,000	
Error	Type I (%)	Type II (%)	Type I (%)	Type II (%)	Type I (%)	Type II (%)	Type I (%)	Type II (%)
Diameter mean	0.3	**5.6**	0.8	*3.2*	0.0	**9.6**	0.0	**6.3**
Diameter max	0.3	**5.1**	0.8	*2.9*	0.0	**8.8**	0.0	**5.7**
Diameter min	0.2	**12.1**	*1.2*	**10.2**	0.0	**21.7**	0.1	**18.7**
ECD	0.8	**7.7**	*1.9*	*4.9*	0.0	**11.0**	0.0	**8.0**
Feret mean	0.4	**6.6**	1.0	*4.0*	0.0	**10.9**	0.0	**7.2**
Feret max	0.3	**5.0**	0.8	*2.8*	0.0	**8.7**	0.0	**5.7**
Feret min	0.2	**12.7**	*1.3*	**10.7**	0.0	**23.0**	0.2	**19.6**
Central distance mean	0.7	**7.9**	*1.8*	**5.8**	0.0	**13.1**	0.0	**10.6**
Central distance max	0.4	**5.2**	0.9	*3.0*	0.0	**8.5**	0.0	**5.0**
Central distance min	*2.5*	**10.6**	*3.3*	**7.9**	**5.2**	**16.6**	*4.1*	**11.8**
Radius of inner circle	0.0	**14.8**	0.2	**13.7**	*1.3*	**32.6**	*1.6*	**27.3**
Perimeter	0.0	**14.4**	0.8	*4.5*	0.0	**23.3**	0.1	**10.0**
Area	0.0	**14.8**	*1.2*	**6.2**	0.0	**28.2**	0.0	**12.6**
Convex area	0.0	**14.9**	0.6	**7.0**	0.0	**32.1**	0.0	**15.7**
Convex perimeter	0.4	**6.6**	1.0	*3.8*	0.0	**10.9**	0.0	**7.4**
Rectangle mean	0.0	**14.9**	0.4	**7.2**	0.0	**31.8**	0.0	**16.0**
Rectangle max	0.0	**14.9**	0.3	**7.1**	0.0	**31.6**	0.0	**15.6**
Rectangle min	0.0	**14.9**	0.6	**8.0**	0.0	**32.2**	0.0	**17.8**
Aspect ratio	0.2	*3.2*	0.3	*2.6*	0.0	**12.3**	0.0	**9.5**
Convexity	1.0	**5.1**	*4.2*	**7.1**	0.2	**8.3**	0.8	**5.9**
Elongation	0.0	*2.7*	0.0	*2.0*	0.0	**12.5**	0.0	**9.7**
Shape factor	*1.2*	*1.9*	**5.3**	**6.8**	0.3	*3.6*	*2.1*	*3.3*
Sphericity	*1.1*	*1.1*	0.9	0.8	*1.1*	*4.9*	0.9	*3.8*

The cells with normal numbers indicate an error of less than 1.0 %, the cells marked with italic numbers indicate an error between 1.0 and 5.0 % and the cells marked with bold numbers indicate an error of more than 5.0 %
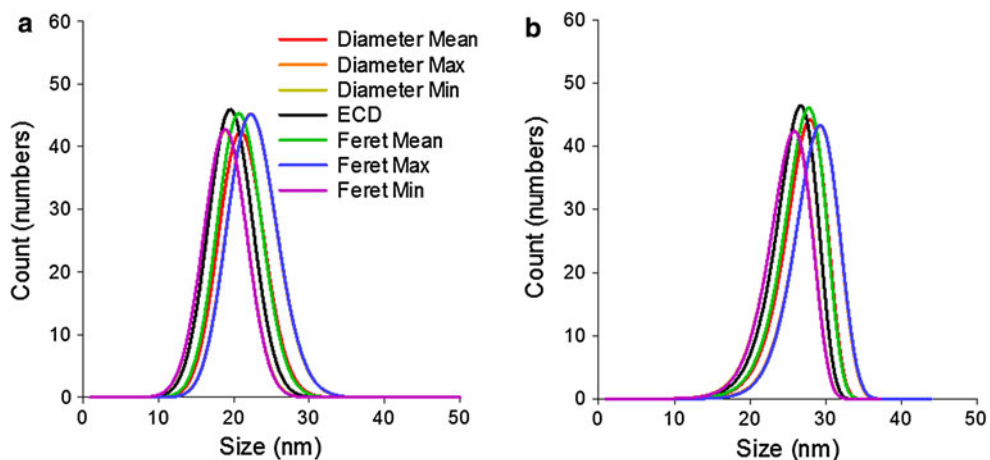
Appendix 5

See Fig. 7.
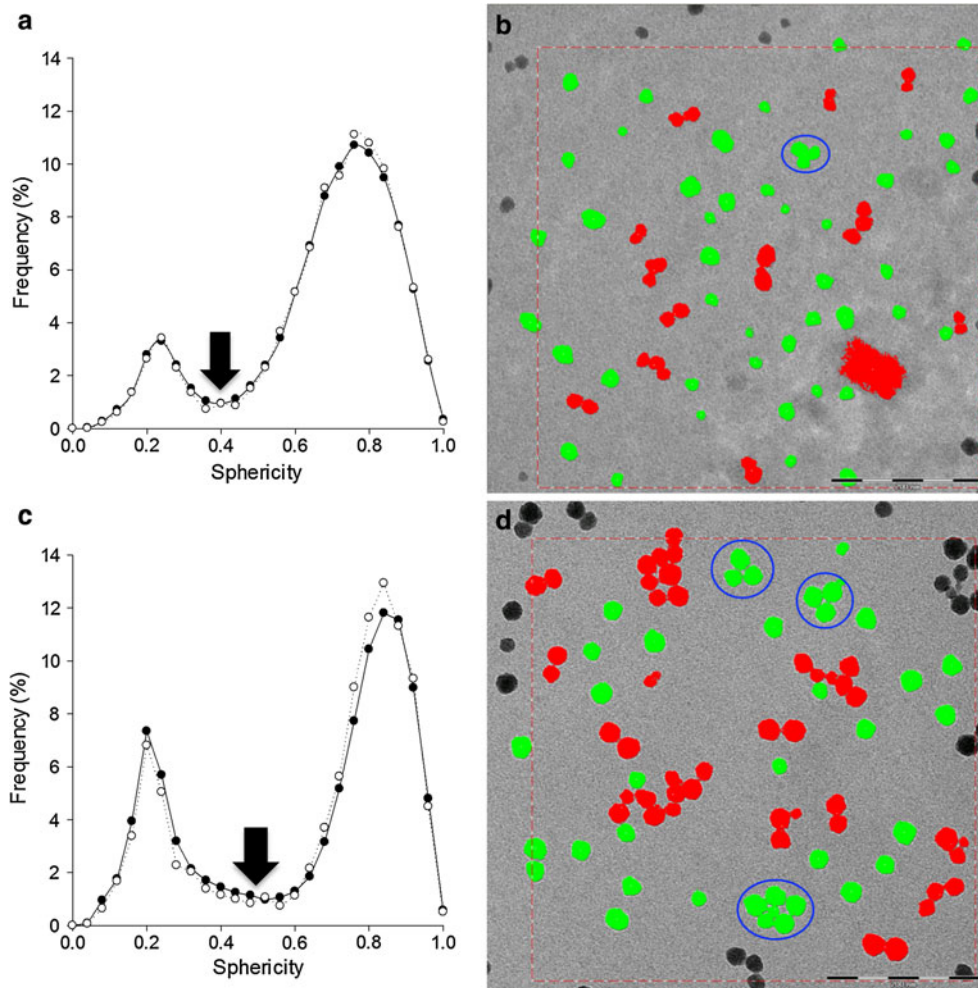
Fig. 7 Comparison of sphericity-based separation of single primary particles and agglomerated primary particles of samples ERM-FD100 and ERM-FD304 at magnifications of 18,500 and 68,000 times. The number-based sphericity distributions of ERM-FD100 and ERM-FD304 at magnifications of 18,500 times (*filled circle*) and 68,000 times (*unfilled circle*) are given in (**a**) and (**c**), respectively. The separation threshold, which separates the primary particles and agglomerates, is set to 0.4 for ERM-FD100 and to 0.5 for ERM-FD304. This threshold is indicated by a *black arrow* in (**a**) and (**c**). Micrographs (**b**) and (**d**) are recorded at a magnification of 68,000 times and illustrate the separation method. Particles in *green* are primary particles with a sphericity higher than 0.4 for ERM-FD100 (**c**) and higher than 0.5 for ERM-FD304 (**d**). Particles with a sphericity lower than these respective thresholds are colored *red*. *Blue circles* indicate the misclassified particles. *Scale bar* corresponds to 200 nm. (Color figure online)

Appendix 6

See Fig. 8.

Fig. 8 Number-based size distributions of ERM-FD100 (**a**) and ERM-FD304 (**b**) at magnification of 68,000 times. The reported fittings are based on the mean values of the mode and FWHM in Appendix 7

Appendix 7

See Table 9.

Table 9 Primary particle mean mode and full width at half maximum (FWHM) of the number-based size distributions and the corresponding intra-laboratory uncertainty u(lab) for ERM-FD100 and ERM-FD304 at magnification of 68,000 times

	ERM-FD100		ERM-FD304	
	Mode $\pm$ u(lab)	FWHM $\pm$ u(lab)	Mode $\pm$ u(lab)	FWHM $\pm$ u(lab)
Diameter mean	20.9 $\pm$ 0.5 nm[a]	7.1 $\pm$ 0.4 nm[a]	27.9 $\pm$ 0.7 nm[a,b]	6.3 $\pm$ 0.4 nm[a]
Diameter max	22.2 $\pm$ 0.5 nm[b]	7.7 $\pm$ 0.4 nm[b]	29.2 $\pm$ 0.7 nm[a,c]	6.7 $\pm$ 0.4 nm[b]
Diameter min	18.9 $\pm$ 0.5 nm[c]	6.8 $\pm$ 0.4 nm[c]	25.9 $\pm$ 0.6 nm[d]	6.4 $\pm$ 0.4 nm[a]
ECD	19.5 $\pm$ 0.5 nm[d]	6.9 $\pm$ 0.4nm[a,c]	26.7 $\pm$ 0.6 nm[b,d]	6.2 $\pm$ 0.5 nm[a]
Feret mean	20.7 $\pm$ 0.6 nm[e]	7.0 $\pm$ 0.5 nm[a]	27.7 $\pm$ 0.6 nm[b,c]	6.3 $\pm$ 0.5 nm[a]
Feret max	22.3 $\pm$ 0.5 nm[b]	7.7 $\pm$ 0.4 nm[b]	29.3 $\pm$ 0.6 nm[a]	6.7 $\pm$ 0.4 nm[b]
Feret min	18.9 $\pm$ 0.5 nm[c]	6.8 $\pm$ 0.4 nm[c]	25.9 $\pm$ 0.5 nm[d]	6.4 $\pm$ 0.4 nm[a]

[a,b,c,d] Different letters indicate significant different mean values by one-way analysis of variance and Tukey test ($p < 0.05$)

Appendix 8

See Table 10.

Table 10 Mean median values of 23 quantitative measurands, their corresponding standard deviations, s, and intra-laboratory uncertainty, u(lab), for ERM-FD100 at magnifications of 18,500 and 68,000 times

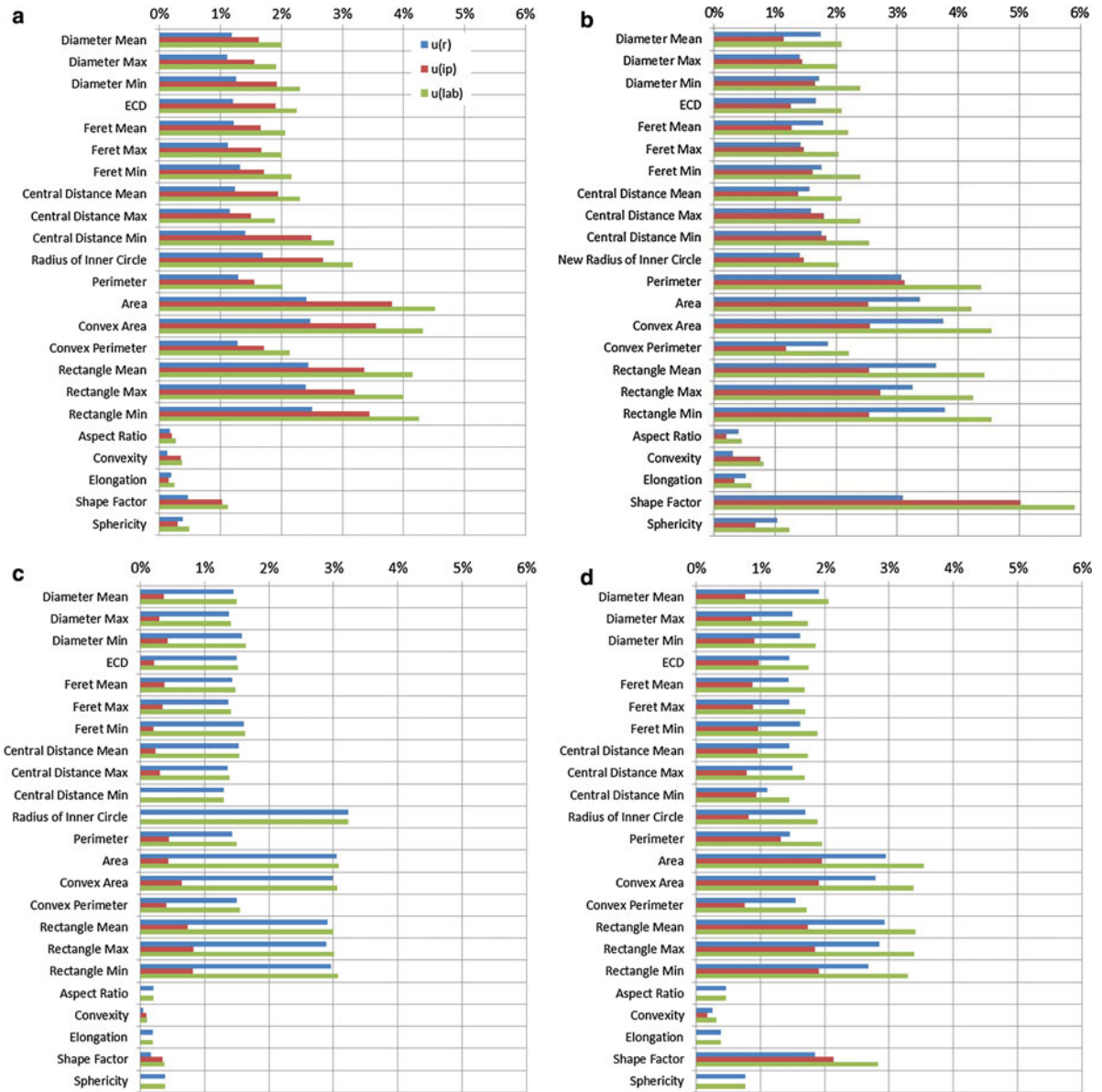| Magnification	18,500 times			68,000 times		
	Mean	s	u(lab)	Mean	s	u(lab)
Diameter mean (nm)	21.2	0.4	0.4	21.1	0.4	0.4
Diameter max (nm)	22.8	0.4	0.4	22.5	0.4	0.5
Diameter min (nm)	19.0	0.4	0.5	18.9	0.4	0.4
ECD (nm)	20.2	0.4	0.5	19.6	0.4	0.4
Feret mean (nm)	21.2	0.4	0.4	20.9	0.4	0.4
Feret max (nm)	22.8	0.4	0.4	22.6	0.4	0.4
Feret min (nm)	19.2	0.4	0.4	18.9	0.4	0.4
Central distance mean (nm)	9.9	0.2	0.2	9.8	0.2	0.2
Central distance max (nm)	11.5	0.2	0.2	11.7	0.3	0.3
Central distance min (nm)	8.2	0.2	0.2	7.8	0.2	0.2
New radius of inner circle (nm)	9.2	0.2	0.3	8.5	0.2	0.2
Perimeter (nm)	66	1	1	73	3	3
Area (nm^2)	320	14	15	303	12	13
Convex area (nm^2)	332	14	15	324	14	14
Convex perimeter (nm^2)	67.3	1.4	1.5	68.4	1.5	1.5
Rectangle mean (nm^2)	448	18	19	434	19	19
Rectangle max (nm^2)	472	18	19	458	19	19
Rectangle min (nm^2)	419	17	18	405	18	18
Aspect ratio	1.161	0.003	0.003	1.166	0.006	0.006
Convexity	0.964	0.003	0.004	0.937	0.007	0.008
Elongation	1.153	0.003	0.003	1.152	0.007	0.007
Shape factor	0.924	0.010	0.011	0.734	0.041	0.043
Sphericity	0.752	0.004	0.004	0.754	0.009	0.010

Appendix 9

See Table 11.

Table 11 Mean median values of 23 quantitative measurands, their corresponding standard deviations, s, and intra-laboratory uncertainty, u(lab), for ERM-FD304 at magnifications of 18,500 times and 68,000 times

Magnification	18,500 times			68,000 times		
	Mean	s	u(lab)	Mean	s	u(lab)
Diameter mean (nm)	27.9	0.4	04	27.3	0.4	0.5
Diameter max (nm)	29.5	0.4	0.4	28.8	0.5	0.5
Diameter min (nm)	25.8	0.4	0.4	25.3	0.5	0.5
ECD (nm)	27.1	0.4	0.4	26.1	0.4	0.5
Feret mean (nm)	28.0	0.4	0.4	27.2	0.4	0.5
Feret max (nm)	29.6	0.4	0.4	28.8	0.5	0.5
Feret min (nm)	26.1	0.4	0.4	25.3	0.5	0.5
Central distance mean (nm)	13.3	0.2	0.2	13.0	0.2	0.2
Central distance max (nm)	14.8	0.2	0.2	14.7	0.2	0.2
Central distance min (nm)	11.6	0.1	0.2	11.0	0.2	0.2
New radius of inner circle (nm)	12.7	0.4	0.4	11.8	0.2	0.2
Perimeter (nm)	87.2	1.3	1.3	92.0	1.7	1.8
Area (nm^2)	575	18	18	536	19	19
Convex area (nm^2)	591	18	18	559	18	19
Convex perimeter (nm^2)	89.7	1.4	1.4	89.1	1.5	1.5
Rectangle mean (nm^2)	781	23	23	737	25	25
Rectangle max (nm^2)	815	24	25	768	26	26
Rectangle min (nm^2)	741	23	23	699	22	23
Aspect ratio	1.110	0.002	0.002	1.117	0.005	0.005
Convexity	0.974	0.001	0.001	0.957	0.003	0.003
Elongation	1.097	0.002	0.002	1.101	0.004	0.004
Shape factor	0.950	0.003	0.004	0.802	0.022	0.023
Sphericity	0.830	0.003	0.003	0.825	0.006	0.006

Appendix 10

See Fig. 9.

Fig. 9 Relative uncertainties (%) for ERM-FD100 at magnification of 18,500 (**a**) and 68,000 times (**b**) and for ERM-FD304 magnification of 18,500 (**c**) and 68,000 times (**d**). For 23 median measured measurands, the repeatability uncertainty is indicated in *blue*; the intermediate precision uncertainty is indicated in *red* and intra-laboratory uncertainty is indicated in *green*. (Color figure online)

References

ASTM E766-98(2008)e1 (2008) Standard practice for calibrating the magnification of a scanning electron microscope. Am Soc Test Mater 49:439–442. doi:10.1520/E0766-98R08E01

Bau S, Witschger O, Gensdarmes F, Rastoix O, Thomas D (2010) A TEM-based method as an alternative to the BET method for measuring off-line the specific surface area of nanoaerosols. Powder Technol 200(3):190–201. doi:10.1016/j.powtec.2010.02.023

Bonas G, Zervou M, Papaeoannou T, Lees M (2003) SoftCRM: a new software for the certification of reference materials. Accred Qual Assur 8(3):101–107. doi:10.1007/s00769-003-0597-9

Braun A, Couteau O, Franks K, Kestens V, Roebben G, Lamberty A, Linsinger TPJ (2011a) Validation of dynamic light scattering and centrifugal liquid sedimentation methods for nanoparticle characterisation. Adv Powder Technol 22(6):766–770. doi:10.1016/j.apt.2010.11.001

Braun A, Franks K, Kestens V, Roebben G, Lamberty A, Linsinger TPJ (2011b) Certified reference material ERM®-FD100: certification of equivalent spherical diameters of silica nanoparticles in water. In: Couteau O (ed) Report EUR 25018 EN. European Union, Luxembourg. doi:10.2787/33725

De Temmerman P-J, Van Doren E, Verleysen E, der Van Stede Y, Francisco M, Mast J (2012) Quantitative characterization of agglomerates and aggregates of pyrogenic and precipitated amorphous silica nanomaterials by transmission electron microscopy. J Nanobiotechnol 10(24):10–24. doi:10.1186/1477-3155-10-24

EC (2011) Commision recommendation of 18 October 2011 on the definition of nanomaterial. Off J Eur Un 275:38–40

EFSA (2011) Scientific opinion: guidance on the risk assessment of the application of nanoscience and nanotechnologies in the food and feed chain. EFSA J 9(5):2140. doi:10.2903/j.efsa.2011.2140

Ehara K, Sakurai H (2010) Metrology of airborne and liquid-borne nanoparticles: current status and future needs. Metrologia 47(2):83. doi:10.1088/0026-1394/47/2/S09

FEI (2012) Tecnai on-line help manual—options. http://www4.utsouthwestern.edu/mcif/manuals/tecnai/Options.pdf

Franks K, Braun A, Charoud-Got J, Couteau O, Kestens V, Lamberty A, Linsinger TPJ, Roebben G (2012) Certified reference material ERM®-FD304: certification of the equivalent spherical diameters of silica nanoparticles in aqueous solution. In: Rasmussen K (ed) EUR 24620 EN. European Union, Luxembourg. doi:10.2787/53476

Freedman D, Diaconis P (1981) On the histogram as a density estimator: L 2 theory. Z Wahrscheinlichkeit 57(4):453–476. doi:10.1007/bf01025868

IRMM (2011) Certificate of analysis ERM®-FD100. Institute for Reference Materials and Measurements, Geel

IRMM (2012) Certificate of analysis ERM®-FD304. Institute for Reference Materials and Measurements, Geel

ISO 13322-1 (2004) Particle size analysis - image analysis methods. Part 1: static image analysis methods. International Organization for Standardization, Geneva

ISO 9276-1 (1998) Representation of results of particle size analysis. Part 1: graphical representation. International Organization for Standardization, Geneva

ISO 9276-2 (2001) Representation of results of particle size analysis. Part 2: calculation of average particle sizes/diameters and moments from particle size distributions. International Organization for Standardization, Geneva

ISO 9276-3 (2008) Representation of results of particle size analysis. Part 3: adjustment of an experimental curve to a reference model. International Organization for Standardization, Geneva

ISO 9276-6 (2008) Part 6: descriptive and quantitative representation of particle shape and morphology. Representation of results of particle size analysis. International Organization for Standardization, Geneva

ISO/IEC GUIDE 98-3 (2008) Uncertainty of measurement. Part 3: guide to the expression of uncertainty in measurement (gum:1995). International Organization for Standardization, Geneva

ISO/TS 27687 (2008) Nanotechnologies—terminology and definitions for nano-objects—nanoparticle, nanofibre and nanoplate. International Organization for Standardization, Geneva

Kaiser DL, Watters RL (2007) Reference material 8012: gold nanoparticles, nominal 30 nm diameter. Report of Investigation. National Institute of Standards & Technology, Gaitersburg

Klein C, Comero S, Stahlmecke B, Romazanov J, Kuhlbusch T, Van Doren E, De Temmerman P-J, Mast J, Wick P, Krug H, Locoro G, Hund-Rinke K, Kördel W, Friedrichs S, Maier G, Werner J, Linsinger TPJ, Gawlik BM (2011) NM-Series of Representative Manufactured Nanomaterials: NM-300 Silver Characterisation, Stability, Homogeneity. EUR 24693 EN—2011. doi:10.2788/23079

Linsinger TPJ (2010) ERM Application Note 1. Comparison of a measurement result with the certified value. European Commission - Joint Research Centre Institution for Reference Materials and Measurements (IRMM), Geel

Linsinger TPJ, Roebben G, Gilliland D, Calzolai L, Rossi F, Gibson N, Klein C (2012) Requirements on measurements for the implementation of the European Commission definition of the term 'nanomaterial'. EUR 25404 EN, Martinsburg. doi:10.2787/63490

Mast J, Demeestere L (2009) Electron tomography of negatively stained complex viruses: application in their diagnosis. Diagn Pathol 4:5. doi:10.1186/1746-1596-4-5

Masuda H, Gotoh K (1999) Study on the sample size required for the estimation of mean particle diameter. Adv Powder Technology 10(2):159–173. doi:10.1163/156855299x00055

Merkus HG (2009) Particle size measurements: fundamentals, practice, quality. Springer, Pijnacker. doi:10.1007/978-1-4020-9016-5

OECD (2010) Guidance manual for the testing of manufactured nanomaterials: OECD sponsorship programme: first revision ENV/JM/MONO(2009) 20/REV. Organisation for Economic Co-operation and Development, Paris

Pons MN, Vivier H, Belaroui K, Bernard-Michel B, Cordier F, Oulhana D, Dodds JA (1999) Particle morphology: from visualisation to measurement. Powder Technol 103(1):44–57. doi:10.1016/s0032-5910(99)00023-6

Pyrz WD, Buttrey DJ (2008) Particle size determination using TEM: a discussion of image acquisition and analysis for the

novice microscopist. Langmuir 24(20):11350–11360. doi:10.1021/la801367j

Roebben G, Rasmussen K, Kestens V, Linsinger TPJ, Rauscher H, Emons H, Stamm H (2013) Reference materials and representative test materials: the nanotechnology case. J Nanopart Res 15(3):1–13. doi:10.1007/s11051-013-1455-2

Russ JC (2011) The image processing handbook. CRC Press, Boca Raton. doi:10.1017/S1431927611012050

SCENIHR (2010) Scientific basis for the definition of the term "Nanomaterial". scenihr_o_032. Scientific committee on emerging and newly identified health risks, Brussels. doi:10.2772/39703

Scott DW (2009) Sturges' rule. WIRes Comp Stat 1:303–306. doi:10.1002/wics.35

Scott DW (2010) Scott's rule. WIRes Comp Stat 2:497–502. doi:10.1002/wics.103

Van Doren E, De Temmerman P-J, Francisco M, Mast J (2011) Determination of the volume-specific surface area by using transmission electron tomography for characterization and definition of nanomaterials. J Nanobiotechnol 9(1):17. doi:10.1186/1477-3155-9-17

Wojdyr M (2010) Fityk: a general-purpose peak fitting program. J Appl Cryst 43:1126–1128. doi:10.1107/S0021889810030499